LETTER

# Impact of Arrival Angle Spread of Each Cluster of Irresolvable Paths on Adaptive Antenna Array and Antenna Diversity in DS-CDMA Mobile Radio

**Yusuke SUZUKI**[†a)], **Eisuke KUDOH**[††b)], ***and*** **Fumiyuki ADACHI**[††c)], ***Members***

**SUMMARY** Adaptive antenna array is a promising technique to increase the link capacity in mobile radio communications systems by suppressing multiple access interference (MAI). In the mobile radio, the received signal consists of discrete paths, each being a cluster of many irresolvable paths arriving from different directions. For large arrival angle spread of each cluster of irresolvable paths, antenna array cannot form a beam pattern that sufficiently suppresses MAI even in the presence of single interference signal and hence, the transmission performance may degrade. In this situation, the use of antenna diversity may be a better solution. It is an interesting question as to which can achieve a better performance, antenna diversity reception or adaptive antenna array. In this letter, we study the impact of the arrival angle spread on the DS-CDMA transmission performances achievable with adaptive antenna array and antenna diversity reception. It is pointed out that the arrival angle spread is an important parameter to determine the performances of adaptive antenna array and antenna diversity.

***key words:*** *adaptive antenna array, mobile communication, DS-CDMA, LMS algorithm, multipath fading*

## 1. Introduction

Transmission links of direct sequence code division multiple access (DS-CDMA) mobile radio are interference-limited due to large multiple access interference (MAI) since all users communicate simultaneously in the same frequency band. Antenna diversity and rake combining are well-known techniques to improve the transmission performance [1]. Another promising technique to suppress the MAI is adaptive antenna array [2]–[5]. The mobile radio channel is a multipath channel consisting of many paths having different time delays. DS-CDMA receiver can resolve the channel into chip-spaced paths (the delay time resolution equals the spreading chip period $T_c$). Each chip-spaced discrete path is a cluster of many irresolvable paths having different time delays of within $\pm 0.5T_c$ from its mean. The arrival angle of each cluster of irresolvable paths may be spread. For small arrival angle spreads, antenna array can sufficiently suppress the MAI. For large arrival angle spreads, however, a beam pattern cannot be formed that suppresses the MAI even in the presence of single interfering signal and the transmission performance of adaptive antenna array may degrade. In this situation, the use of antenna diversity may be a better solution. An interesting question is which achieves a better performance: antenna diversity reception or adaptive antenna array.

In this letter, as a preliminary study, 2-branch antenna case is assumed and we study the difference in the impact of the arrival angle spread of each cluster of irresolvable paths on the DS-CDMA transmission performances achievable with adaptive antenna array and antenna diversity reception. The remainder of this letter is organized as follows. In Sect. 2, the propagation model is presented. Section 3 presents the transmission model. Section 4 evaluates the bit error rate (BER) performance by computer simulation. Section 5 gives some conclusions.

## 2. Propagation Model

In this letter, we assume a 2-antenna mobile receiver in the presence of one interfering base station for the DS-CDMA downlink (base-to-mobile) and a multipath channel having $L$ discrete paths. Figure 1 illustrates the model of incoming desired and interfering signals when $L$=2, where subscripts $s$ and $i$ denote the desired and the interfering signals, respectively, and $d$ represents the antenna separation. The $l$-th discrete path ($l = 0 \sim L-1$) is a cluster of many irresolvable paths whose arrival angles are assumed to be Gaussian distributed around its central arrival angle $\phi_l$ with the standard deviation of $\Delta$ (this is simply called the multipath arrival angle spread here). The central arrival angle $\phi_l$ is assumed to be uniformly distributed over the angle interval of $[\bar{\phi} - \delta\phi, \bar{\phi} + \delta\phi]$ for all $l$, where $\bar{\phi}$ is called the nominal arrival angle.

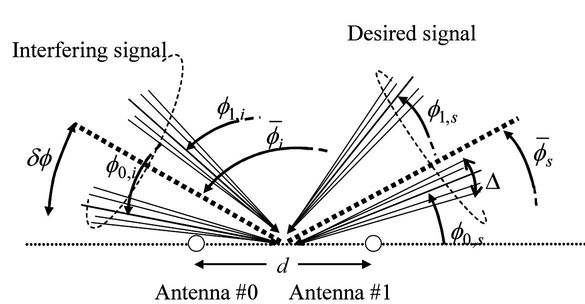


**Fig. 1** Model of incoming desired and interfering signals when $L$=2.

Manuscript received June 27, 2003.
Manuscript revised October 20, 2003.

[†]The author is with Tokyo Electric Construction Office, East Japan Railway Company, Tokyo, 151-8512 Japan.
[††]The authors are with the Department of Electrical and Communication Engineering, Graduate School of Engineering, Tohoku University, Sendai-shi, 980-8579 Japan.
a) E-mail: yusuke-suzuki@jreast.co.jp
b) E-mail: kudoh@mobile.ecei.tohoku.ac.jp
c) E-mail: adachi@ecei.tohoku.ac.jp

## 3. Transmission Model for Pilot-assisted Coherent Adaptive Antenna Array

The pilot-assisted coherent adaptive antenna array [4] is assumed. Figure 2 illustrates its receiver structure. Different antenna beam is formed for each discrete path. The signal output from each beam former is coherently rake combined based on the maximal ratio combining (MRC) [6] method. As Fig. 3 shows, known $N_p$-pilot symbols are periodically time-multiplexed with $N_d$-data symbols; slot length $N_{slot}$ is given by $N_{slot} = N_p + N_d$. The pilot symbols are not only used as the reference signal for adaptive beam forming but also for channel estimation used in coherent detection. Before rake combining, the combining weight $1/\sigma_l^2$ is introduced, where $\sigma_l^2$ denotes the average interference plus noise power, to perform MRC under the condition of different average interference plus noise powers [6].

### 3.1 Signal Representation

The sum of the desired and interfering signals and the additive white Gaussian noise (AWGN) is received on each antenna. The received signal $r^{(j)}(t)$ associated with the $j$-th antenna is given by

$$\begin{aligned} r^{(j)}(t) \;=\;& \sqrt{2P_s}\sum_{l=0}^{L-1}\xi_{s,l}^{(j)}(t)d_s(t-\tau_{s,l})c_s(t-\tau_{s,l}) \\ &+\sqrt{2P_i}\sum_{l=0}^{L-1}\xi_{i,l}^{(j)}(t)d_i(t-\tau_{i,l})c_i(t-\tau_{i,l}) \\ &+n^{(j)}(t) \end{aligned} \quad (1)$$

for $j$=0 and 1, where $P$ is the average received signal power and $\xi(t)$ is the path gain, the subscripts $s$ and $i$ denote the desired and the interfering signals, respectively, $d(t)$ is the data modulated signal waveform and $c(t)$ is the spreading chip waveform. $d(t)$ and $c(t)$ are given by

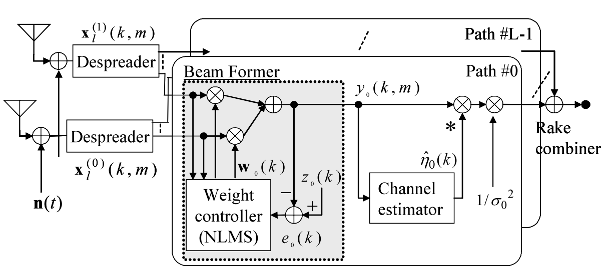


**Fig. 2** Receiver structure.

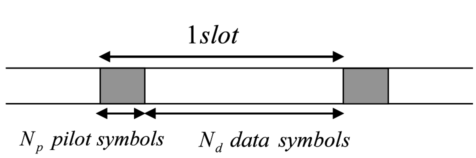


**Fig. 3** Transmission of pilot symbols.

$$\begin{cases} d(t) = \displaystyle\sum_{k=-\infty}^{\infty}\sum_{m=0}^{N_{slot}-1} d_{k,m}u(t/T-(kN_{slot}+m)) \\ c(t) = \displaystyle\sum_{q=-\infty}^{\infty} c_q u(t/T_c-q) \\ u(t) = \begin{cases} 1 & \text{if } 0\le t<1 \\ 0 & \text{otherwise} \end{cases} \end{cases}, \quad (2)$$

where $\{d_{k,m} = \pm 1; k = -\infty \sim +\infty, m = 0 \sim N_{slot}-1\}$ is the data-modulated symbol sequence with $k$ and $m$ representing the slot index and the symbol position in a slot, $\{c_q = \pm 1; q = -\infty \sim +\infty\}$ is the spreading chip sequence, $T$ is the data symbol period, $T_c$ is the spreading chip period, and $u(t)$ is the unit pulse waveform given by $u(t)$=1 for $t = 0 \sim 1$ and 0 otherwise. $SF = T/T_c$ is the spreading factor defined as the number of chips per data symbol. In Eq. (1), $n^{(j)}(t)$ is the zero-mean complex Gaussian noise process with a variance of $2N_0/T_c$, where $N_0$ is the single-sided power spectrum density of the AWGN. The received signal $r^{(j)}(t)$ is multiplied by the spreading sequence. The despreader output for the $m$-th symbol in the $k$-th slot associated with the $l$-th discrete path is denoted by $x_l^{(j)}(k,m)$. The array input signal vector, the antenna weight vector, and the array output signal are denoted by $\boldsymbol{x}_l(k,m)$, $\boldsymbol{w}_l(k)$, and $y_l(k,m)$, respectively, and are given by

$$\begin{cases} \boldsymbol{x}_l(k,m) = [x_l^{(0)}(k,m), x_l^{(1)}(k,m)]^T \\ \boldsymbol{w}_l(k,m) = [w_l^{(0)}(k,m), w_l^{(1)}(k,m)]^T \\ y_l(k,m) = \boldsymbol{x}_l(k,m)^T\boldsymbol{w}_l(k,m) \end{cases}, \quad (3)$$

where $(\cdot)^T$ denotes the transpose matrix. The path gain $\sqrt{2P_s}\xi_{s,l}^{(j)}$ is estimated using a simple averaging filter. Assuming pilot symbol of $p = 1 + j0$, the estimated path gain $\hat{\eta}_l(k)$ is given by

$$\hat{\eta}_l(k) = \frac{1}{N_p}\sum_{m=0}^{N_p-1} y_l(k,m). \quad (4)$$

The coherent rake combiner output $y(k,m)$ is given by

$$y(k,m) = \sum_{l=0}^{L-1}\frac{\hat{\eta}_l^*(k)}{\sigma_l^2}y_l(k,m) \quad (5)$$

for $m = N_p \sim N_{slot}-1$, where * denotes the complex conjugate operation and $\sigma_l^2$ is the average interference plus noise power associated with the $l$-th discrete path. $\sigma_l^2$ is estimated by a first order filter:

$$\sigma_l^2(k) = \alpha\sigma_l^2(k-1) + (1-\alpha)\frac{1}{2}|e_l(k)|^2, \quad (6)$$

where $e_l(k)$ represents the error signal defined later and $\alpha$ is the forgetting factor ($\alpha$ =0.999 is used in the simulation).

### 3.2 Adaptive Beam Forming

Normalized least mean square (NLMS) algorithm is used. In NLMS, $\boldsymbol{w}_l(n)$ is updated as follows [7]

$$\begin{cases} \boldsymbol{w}'_l(n) = \boldsymbol{w}_l(n-1) + 2\mu e_l(n) \dfrac{\boldsymbol{x}_l^*(n)}{\|\boldsymbol{x}_l(n)\|^2} \\ w_l^{(j)}(n) = \dfrac{w'^{(j)}_l(n)}{\|\boldsymbol{w}'_l(n)\|} \end{cases}, \quad (7)$$

where $\boldsymbol{w}_l(n)$ is the weight vector after normalization (the weight normalization is introduced to prevent the divergence), $e_l(n)$ and $\|\boldsymbol{x}_l(n)\|^2$ are the error signal and the square norm of $\boldsymbol{x}_l(n)$, respectively. They are given by

$$\begin{cases} e_l(n) = y_l(n) - z(n) \\ \|\boldsymbol{x}_l(n)\|^2 = \sum_{j=0}^{1} \left| x_l^{(j)}(n) \right|^2 \end{cases}, \quad (8)$$

where $z(n)$ is the reference signal. The choice of the reference signal is important. If the pilot signal is used as the reference signal, the weight vector must track the variations in the path gains. However, this is difficult to achieve in a fast fading environment. Hence, we use the pilot $p$ multiplied by the estimated path gain as in the reference [5], i.e.,

$$z(n) = \hat{\eta}_l(n)p. \quad (9)$$

## 4. Computer Simulation

An $L$=2-path Rayleigh fading having equal average power is considered with the time delay separation between 2 paths being one chip ($1T_c$). It is assumed that binary phase shift keying (BPSK) is used for data modulation, the path gains stay constant over one BPSK symbol period $T$, and the spreading factor $SF$=16. Antenna separation for adaptive antenna array is 0.5 carrier wave length ($\lambda$), i.e., $d = \lambda/2$, however, the antenna separation for antenna diversity reception is varied from $\lambda/2$ to $20\lambda$. $N_p$=4 and $N_d$=60 are assumed. The NLMS algorithm uses the step size $\mu$=0.001. The initial values of antenna weights are set to $w_l^{(0)} = 1$ and $w_l^{(1)} = 0$, i.e., the omni directional antenna.

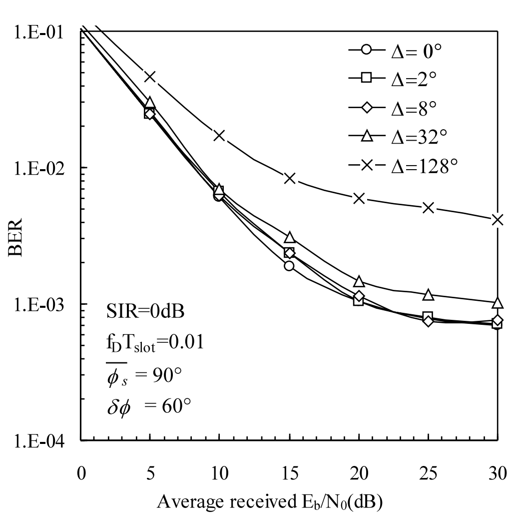


**Fig. 4** The BER performance of adaptive antenna array with Δ as a parameter.

### 4.1 Impact of Multipath Arrival Angle Spread Δ

Figure 4 plots the average BER performance with Δ as a parameter for $\bar{\phi}_s$ =90° and $\delta\phi$ = 60°. The average signal-to-interference power ratio (SIR), defined as $P_s/P_i$, is assumed

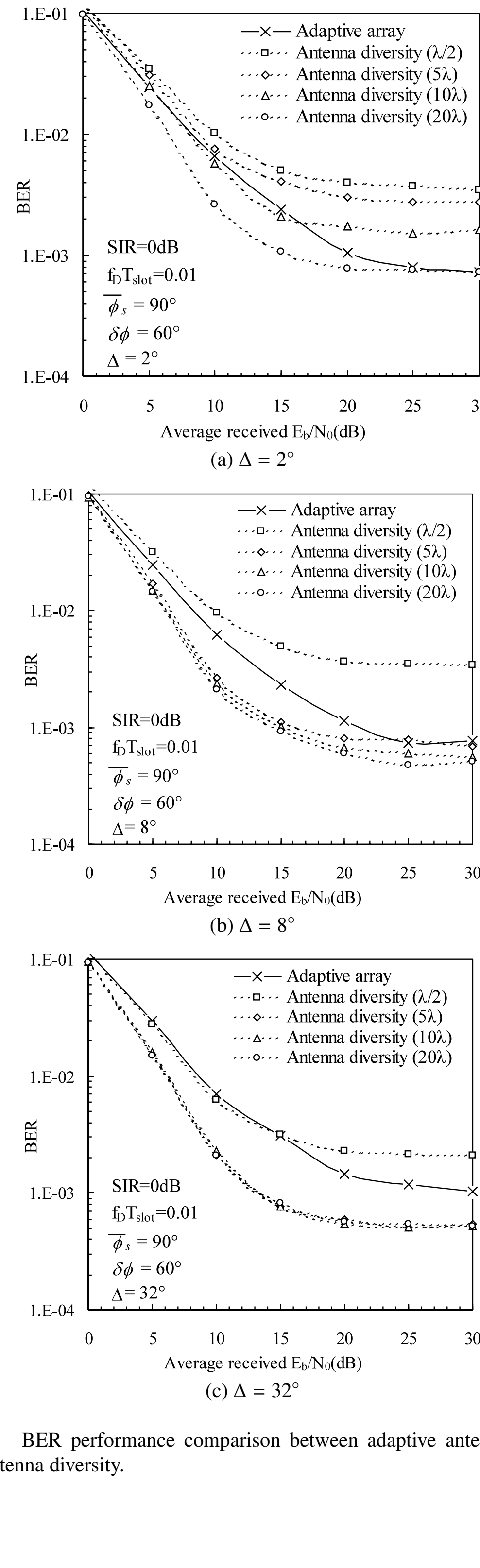


**Fig. 5** BER performance comparison between adaptive antenna array and antenna diversity.

to be 0 dB. When $\Delta < 32°$, since the beam null can be directed toward the direction of interference, the BER performance is not so degraded. However, when $\Delta > 32°$, the BER performance starts to degrade, since a beam pattern that sufficiently suppresses interfering signals cannot be formed.

### 4.2 Comparison with Antenna Diversity

Figure 5 compares the BER performances of adaptive antenna array and antenna diversity for $\Delta = 2°$, 8° and 32°. For antenna diversity reception, various values of antenna separation $d$ are considered. As $\Delta$ becomes larger, the BER performance with antenna diversity improves, while that with adaptive antenna array degrades. This is because, as $\Delta$ increases, the fading correlation between two diversity antennas becomes smaller for the given antenna separation. When $\Delta = 2°$ (8°), antenna diversity provides better BER performance if antenna separation of more than $20\lambda$ ($5\lambda$) is used.

## 5. Conclusions

In this letter, we compared, by computer simulation, the DS-CDMA downlink transmission performances with 2-branch adaptive antenna array and antenna diversity reception with the multipath arrival angle spread $\Delta$ of each cluster of irresolvable paths as a parameter. It was pointed out that the arrival angle spread is an important parameter to determine the performances of adaptive antenna array and antenna diversity. $\Delta$ strongly influences whether adaptive antenna array or antenna diversity reception provides a better BER performance. As $\Delta$ becomes larger, the BER performance with adaptive antenna array degrades. However, when $\Delta < 32°$, the BER performance with adaptive antenna array does not degrade so much, since the beam null can be directed toward the direction of interference. On the other hand, the BER performance with antenna diversity reception consistently improves as $\Delta$ increases. When $\Delta = 2°$ (8°), antenna diversity reception provides better BER performance than adaptive array if antenna separation is larger than $20\lambda$ ($5\lambda$). The above results are for the case of two antennas. The performance comparison of adaptive antenna array and antenna diversity for the case of more than two antennas is an interesting topic to study.

**References**


[1] F. Adachi, M. Sawahashi, and H. Suda, "Wideband DS-CDMA for next-generation mobile communications systems," IEEE Commun. Mag., vol.36, no.9, pp.56–69, Sept. 1998.

[2] L.C. Godara, "Application of antenna arrays to mobile communications, Part I: Performance improvement, feasibility, and system considerations," Proc. IEEE, vol.85, no.7, pp.1029–1060, July 1997.

[3] L.C. Godara, "Application of antenna arrays to mobile communications, Part II: Beam-forming and direction of arrival consideration," Proc. IEEE, vol.85, no.8, pp.1195–1245, Aug. 1997.

[4] S. Tanaka, M. Sawahashi, and F. Adachi, "Pilot symbol-assisted decision-directed coherent adaptive array diversity for DS-CDMA mobile radio reverse link," IEICE Trans. Fundamentals, vol.E80-A, no.12, pp.2445–2454, Dec. 1997.

[5] Y. Suzuki, E. Kudoh, and F. Adachi, "Effect of the reference signal used for updating the weight of adaptive antenna array on the beam pattern," IEICE Technical Report, RCS2002-146, Aug. 2002 (in Japanese).

[6] M. Schwarz, W.R. Bennett, and S. Stein, Communication Systems and Techniques, McGraw-Hill, New York, 1966.

[7] S. Haykin, Adaptive Filter Theory, 3rd ed., Prentice Hall, Englewood Cliffs, 1996.